JOURNAL OF GEOPHYSICAL RESEARCH, VOL. 102, NO. B2, PAGES 2953–2967, FEBRUARY 10, 1997

Upper mantle compressional velocity structure beneath the West Mediterranean Basin

N. Alessandro Pino
Istituto Nazionale di Geofisica, Rome, Italy

Donald V. Helmberger
Seismological Laboratory, California Institute of Technology, Pasadena

Abstract. *P* waveforms of regional crustal earthquakes have been modeled to obtain an upper mantle compressional velocity model for the West Mediterranean Basin. Data come from long-period stations of the World-Wide Standardized Seismograph Network and broadband stations located in the Iberian Peninsula. Synthetic waveforms have first been computed for published velocity models corresponding to different tectonic provinces and obtained with analogous techniques. A model that strongly improves the fits to the data is then derived. The proposed model is characterized by a 100-km-thick lid overlaying a not very pronounced low-velocity zone and a 3% discontinuity at 368 km where an increase of the velocity gradient also occurs. These features could be explained either as a deflection of the olivine-to-spinel phase transition, regionally detected at about 395 km, resulting from the lower temperature produced by the subduction of the African plate, or as being due to the presence below 300 km depth of a layer of silicate melt, producing a strong reflection from its bottom, and a more usual depth for the olivine-spinel transition. In both cases the occurrence of relatively low velocities beneath 300 km is interpreted as being caused by the presence of melt associated with the northward dipping subduction of the African plate.

Introduction

The tectonic activity in a region is strongly correlated to the physical and chemical properties of the underlying upper mantle. Many studies have pointed out that major differences in the seismic velocity structure between shield and tectonically active regions are confined to the upper 400 km [e.g., *Grand and Helmberger,* 1984]. A detailed knowledge of the upper mantle structure is then crucial to a full comprehension of processes like subduction and seafloor spreading.

In the last decade, several papers that try to assess the petrology of the upper mantle using seismic velocity models have been published (see, for instance, *Anderson and Bass* [1984], *Duffy and Anderson* [1989], and *Ita and Stixrude* [1992] for the upper mantle and the transition zone). Thus the determination of the seismic structure may help constrain the mantle's composition and thermodynamic state.

The western Mediterranean region is characterized by a highly complex tectonic environment as testified by its surface geology and seismicity. In the last 175 Myr it has experienced several phases of motion, with reversal in the direction of the relative motion between Africa and Europe, counterclockwise rotation of the Corsica-Sardinia block, formation of the Apenninic chain, opening of the Tyrrhenian and Balearic oceanic basins, and subduction in the southern Tyrrhenian Sea [*Dewey et al.*, 1989]. This intricate tectonic evolution has resulted in a complex crustal structure, with patches of oceanic crust in the Balearic [*Hirn et al.*, 1977] and Tyrrhenian Basins [*Steinmetz et al.*, 1983] surrounded by the continental and transitional crust of Europe, Africa, and the Iberian and Italian Peninsulas.

Many seismological studies of the upper mantle in the European-Mediterranean area have been carried out using different approaches. In particular, tomographic models have been obtained from teleseismic [*Romanowicz*, 1980; *Granet and Trampert*, 1989], regional [*Spakman*, 1991], and both regional and teleseismic [*Spakman et al.*, 1993] *P* wave travel times, and on a smaller scale, travel time tomography has been performed for areas of special interest, such as the Hellenic subduction zone [*Papazachos and Nolet*, 1997] or the Italian region [*Scarpa*, 1982; *Amato et al.*, 1993]. Several models for the upper mantle structure based on studying surface wave dispersion curves [*Payo*, 1967; *Berry and Knopoff*, 1967; *Cara et al.*, 1980; *Marillier and Mueller*, 1985], modeling body wave travel time data [*Lehmann*, 1959, 1961; *Bottari and Ghirlanda*, 1974; *England and Worthington*, 1977], or combining the two approaches [*Payo*, 1969; *Mayer-Rosa and Mueller*, 1973; *Panza et al.*, 1980] have also been published; *Snieder* [1988] and *Zielhuis and Nolet* [1994] derived lateral variations of the shear wave velocity in the upper mantle from surface wave and surface and long-period *S* waveform inversion, respectively. In a few cases, forward modeling using either long-period *P* [*Burdick*, 1981] or broadband [*Paulssen*, 1987] body waveforms by computing synthetic seismograms has been applied.

First arrival travel time tomography is especially suitable to provide maps of relative velocity, but it requires a high density of both earthquakes and stations. Owing to the geometry of ray paths, vertical resolution in the upper mantle is generally of the order of 100 km at best, and in the western Mediterranean region this resolution is very poor particularly in the central part of the

Paper number 96JB03461.
0148-0227/97/96JB-03461$09.00

basin. Moreover, since only travel times are utilized, no detailed information about the amplitude of velocity discontinuities can be deduced from tomographic inversion, and their location in depth is usually a fixed parameter in the procedure. Surface wave studies, namely, dispersion curves and waveform inversion, have even lower resolution.

Forward modeling is widely applied as a method for interpreting the different seismic phases and for determining the absolute values of seismic velocities. This technique allows a direct test of the effects that different structural features produce on waveforms. Once the model space has been extensively explored to determine the gross structure, this can be refined by finely fitting the waveforms; investigation of small-scale heterogeneities is then possible, and the existence of discontinuities, their depth, and their magnitude can be resolved with some accuracy.

In the last decade, several upper mantle models for different regions have been obtained by matching body waveforms from regional earthquakes with synthetic seismograms in horizontally stratified media [e.g., *Zhao and Helmberger*, 1993]. As long as paths associated with the same tectonic province (pure paths) are being considered, the resulting model may represent a reliable image of the actual velocity-depth distribution. However, even if laterally inhomogeneous structures are analyzed, this approach can provide information on the degree of lateral heterogeneity [*Paulssen*, 1987].

In spite of the relatively large number of studies of the upper mantle structure in the western Mediterranean region, uncertainties concerning mainly the lithosphere-asthenosphere system, the velocity gradient, and the magnitude and depth of the "410-km" discontinuity still persist. Indeed, this is one of the most anomalous regions sampled in the global study by *Shearer* [1993], who performed a mapping of upper mantle reflectors from long-period precursors to *SS* phase. He sees a strong reflector at about 360 km depth with little evidence for the nearly universal 410-km discontinuity.

In this study we address this issue, by performing a detailed analysis of *P* waveform triplication data. First, we compare our waveform data against predictions based on other regionalized models. Then we determine a new model following a trial-and-error approach which has proven effective in other regions.

Data

Upper mantle structure produces triplications in *P* phases at distances of up to 30°; in general, first arrivals correspond to rays bottoming in the uppermost 400 km at epicentral distances of up to 17°, for tectonic structures, or of up to 19° for shield ones [*Burdick*, 1981]. At distances of less than 10°, *P* wave trains are dominated by the longer-period *PL* phase, confined to the crustal wave guide, which can contaminate seismograms [*Helmberger*, 1972]. In order to model the upper 400 km, data recorded in the range 12° through 17°-19° should then be considered. The magnitude of the earthquakes should be large enough to produce a high signal-to-noise ratio, but not much larger if source complexities (finiteness of fault plane, directivity, complex source time function, etc.) that can considerably affect waveforms and introduce more unknown parameters are to be avoided.

Among the 5.0-6.0 magnitude earthquakes that occurred in the studied area over the period 1977-1990, we have selected the best recorded events in the region which satisfied the above conditions (Table 1). Since all of them are located to the east of the West Mediterranean Basin, in the former Yugoslavia and along the Italian and Balkan Peninsulas, in this study we use World-Wide Standardized Seismograph Network (WWSSN) LP stations located in the Iberian Peninsula. Figure 1 shows the location of both stations and events and the source-to-receiver great circle paths. All the events are located in the crust along the tectonic margin between the African and the Eurasian plates.

Waveform Modeling

Preliminary Analysis

We have computed synthetic seismograms in one-dimensional structures by applying a method based on generalized ray theory [*Helmberger*, 1983] and convolved with the instrument response. Anelastic attenuation has been accounted for by using the Q Futtermann operator [*Futtermann*, 1962], with a t^* value of 1.5.

Table 1. Earthquakes

Event	Date	Time, UT	Latitude, °N	Longitude, °E	Depth, km	m_b
1	April 3, 1969	2212:23.8	40.500	19.900	18.	5.1
2	May 24, 1979	1723:18.1	42.255	18.752	8.	5.8
3	Sept. 19, 1979	2135:37.2	42.812	13.061	16.	5.9
4	Dec. 8, 1979	0406:34.3	38.284	11.741	33.	5.4
5	May 18, 1980	2002:57.5	43.294	20.837	9.	5.7
6	May 28, 1980	1951:19.3	38.482	14.252	12.	5.7
7	Nov. 25, 1980	1828:21.5	40.660	15.450	15.	4.9
8	Aug. 13, 1981	0258:11.9	44.849	17.312	16.	5.4
9	March 23, 1983	2351:06.5	38.294	20.262	19.	5.8
10	May 7, 1984	1749:41.6	41.765	13.898	10.	5.5
11	May 13, 1984	1245:55.8	42.967	17.734	30.	5.1
12	Oct. 11, 1986	0900:13.1	37.96	28.59	24.	5.4
13	April 27, 1989	2306:51.4	37.06	28.29	10.	5.3
14	April 28, 1989	1330:17.9	37.01	28.25	11.	5.1
15	May 5, 1990	0721:19.4	40.75	15.85	26.	5.3
16	July 18, 1990	1129:23.9	37.00	29.64	10.	5.2
17	April 30, 1992	1144:38.6	35.07	26.71	17.	5.7

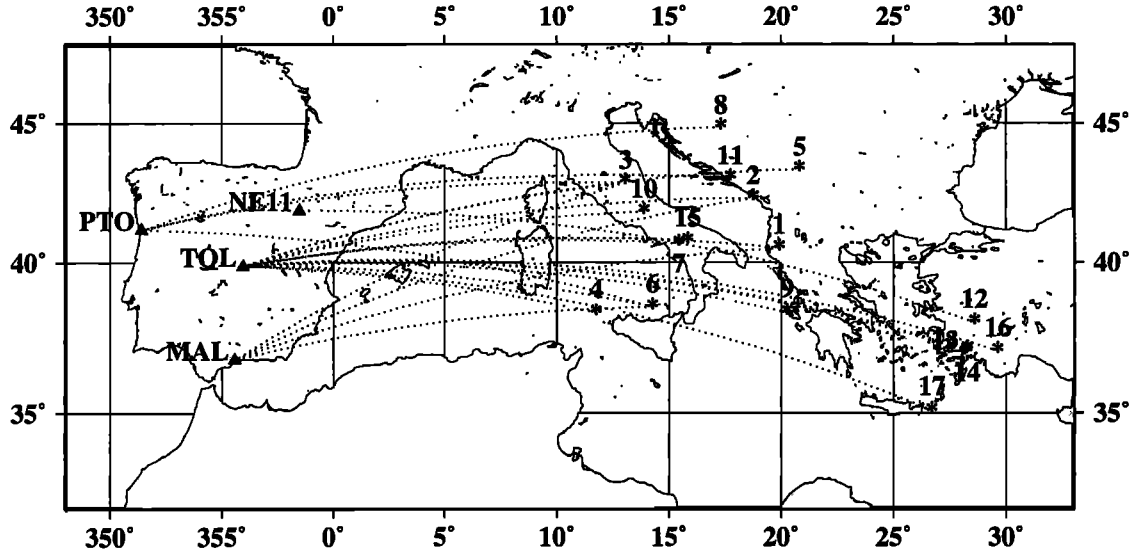

Figure 1. Map of the studied area with event (asterisks) and station (triangles) locations. Source-to-receiver great circle paths are also shown.

For almost all the events, source parameters have been taken from *Anderson and Jackson* [1987]. They used first motion polarities and teleseismic waveform modeling to determine fault plane solutions and assumed the ISC or NEIS locations and origin times. For events not included in their study, we have adopted the NEIS location and the source mechanism from the Harvard centroid moment tensor (CMT) catalogue.

We have obtained first-order information on the compressional velocity structure by computing synthetic seismograms for published models which are appropriate for different tectonic regions (Figure 2). S25 was obtained by *LeFevre and Helmberger* [1989] for eastern Canada and is characteristic of stable continental regions; ATLP was recently obtained by *Zhao and Helmberger* [1993] for the upper mantle structure beneath the northwestern Atlantic Ocean and is appropriate for regions having an old oceanic crust (70 to 150 Ma); T9, which is typical of a tectonically active region, was used by *Burdick* [1981] to model North Aegean earthquakes recorded in Spain, spanning approximately the same area considered in this study, but with a minimum epicentral distance of 18°. These models display major differences in the lithosphere-asthenosphere system having lid thicknesses ranging from 30 km to 150 km and in the low-velocity zones; at depths around 400 km, all exhibit a first-order velocity discontinuity of about 5%.

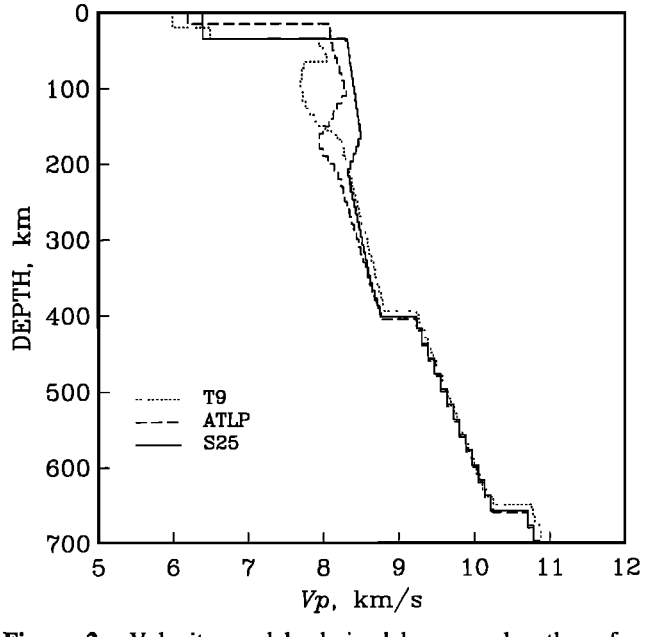

Figure 2. Velocity models derived by several authors for different tectonic provinces: T9 has been obtained by *Burdick* [1981] for the West Mediterranean Basin; ATLP by *Zhao and Helmberger* [1993] for the northwestern Atlantic Ocean; and S25 by *LeFevre and Helmberger* [1989] for the Canadian Shield.

Figure 3 shows a comparison of synthetic seismograms computed for the three models. At all distances under consideration, absolute travel times are shorter for stable continental regions than for tectonic and old ocean ones. Because of the presence of a thin lid and a high-velocity gradient below it, the first arrivals for T9 (A branch) are formed by phases bottoming in the low-velocity layer, while strong lithospheric phases result for S25. The multiple arrival observed in ATLP waveforms up to 18° is composed of phases that propagated in the relatively thick lid (P_n) and a longer-period arrival generated by rays bottoming below 200 km depth (A branch), the time delay between the two phases being controlled by the relative velocity in the lid and the low-velocity layer.

Relative to ATLP-like and T9-like structures, the lower the velocity in the asthenosphere, the shorter are C-A times, since rays bottoming at shallower depths have longer paths in the low-velocity zone than those reflected by the "410-km" discontinuity. The opposite holds for shield structures, because the A branch is due to phases traveling entirely in the lithosphere.

Figure 4 shows data and synthetics computed for S25, ATLP, and T9. It should be noticed that waveforms have been shifted along the time axes in order to align first arrivals. In all models we have used an identical simplified two-layered 30-km-thick crust, representing an average value for the crust in the source and receiver [*Geiss*, 1987] regions. However, at this stage, we focused

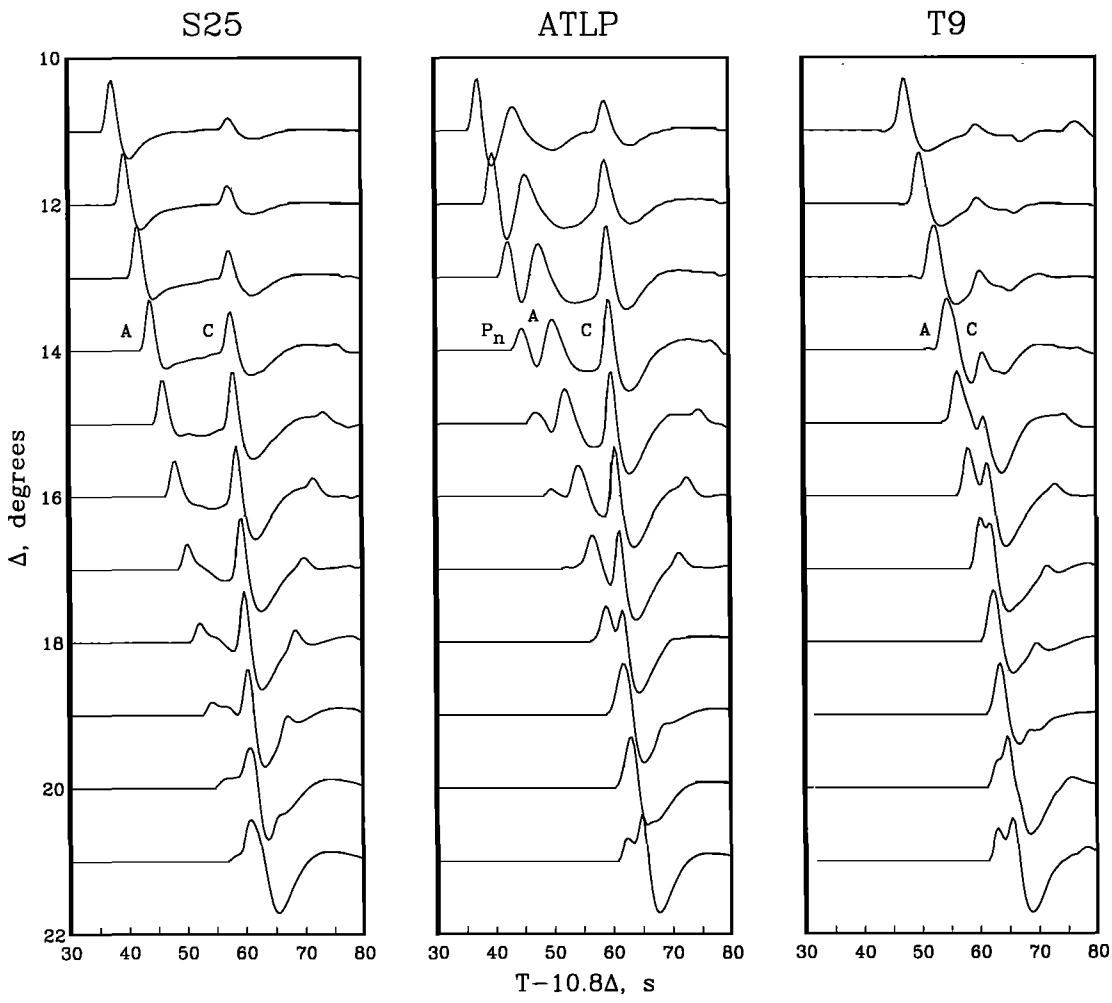

Figure 3. WWSSN-LP synthetics predicted by S25, ATLP, and T9 for the range 11°-21°. Letters indicate different branches of the triplication.

our attention on the relative timing and amplitudes rather than on absolute travel times, and in the ranges under consideration, crustal thickness only affects the latter. Incidentally, compared to the other models, ATLP (with the modified crust) is more effective in predicting first arrival times, with respect to the other models.

None of the above models give good fits to the data. Nevertheless, some conclusions about the upper mantle structure of the area under study can be made. The longer pulse duration in the recorded waveforms, in some cases of about 10 s (10-TOL), is likely to be due to a structural effect rather than to source duration. The magnitudes m_b of the events are between 4.9 and 5.9; for Apenninic events in this range of magnitude, *Cocco and Rovelli* [1989] obtained corner frequencies f_c larger than 0.38 Hz, which gives rupture durations τ shorter than 2.7 s, if $\tau = 1/f_c$ is assumed. On the other hand, the superposition of direct and free surface reflections, *pP* and *sP*, cannot be invoked to explain the long source durations because this effect is also evident on deep crust events (4-TOL), where these arrivals are well separated in time.

Since travel times can hardly be explained by phases traveling in a low-velocity layer or below it, this feature has been interpreted as being due to the constructive interference of the P_n and A branches, produced by an ATLP-like structure. Nevertheless, looking at the waveforms predicted by ATLP, it is also evident that, in order to reduce the relative travel time between these two branches, a faster and/or thinner low-velocity zone should be used.

The arrival usually associated with the "410" discontinuity becomes apparent in the data beyond about 16°, i.e., 3-PTO. In this frame, S25 predicts large C-A travel times, while short C-A times result from T9, which also gives incorrect relative amplitudes, while ATLP gives better fits of relative travel times and amplitudes for all the station-event couples. These results strongly suggest the presence of a moderately thick lid, producing P_n arrivals, overlying a low-velocity layer.

Results

According to the indications obtained by comparing observed with synthetic seismograms computed for the three models under consideration, starting with ATLP as an initial guess, we have developed, by a trial-and-error approach, a one-dimensional model which provides much better fits to the data. In order to overcome problems connected with possible errors in source parameters or with strong lateral heterogeneities transverse to the propagation plane, we have first calibrated the *P* velocity structure to model the waveforms of event 3, as recorded at the

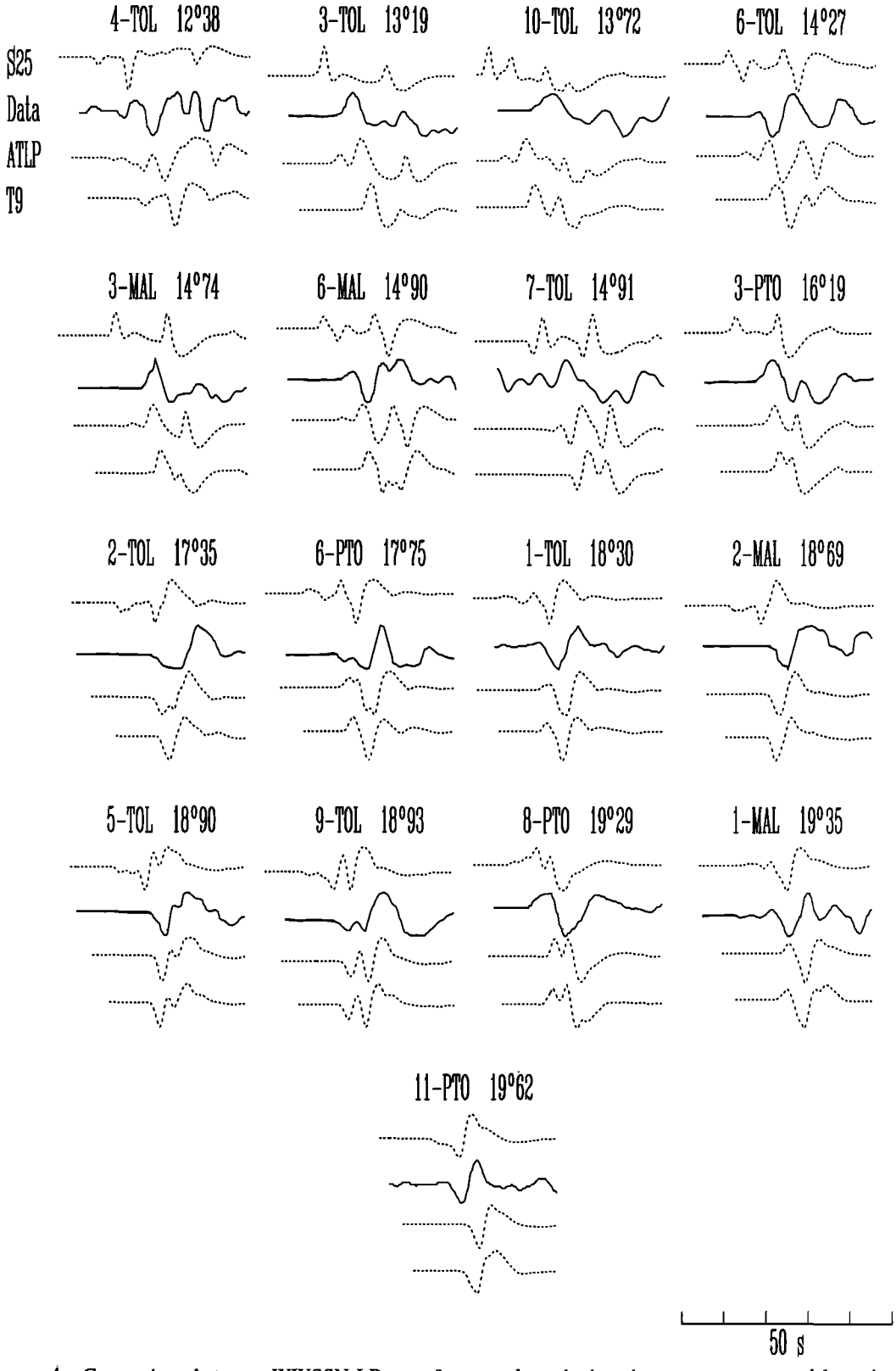

Figure 4. Comparison between WWSSN-LP waveforms and synthetic seismograms computed by using the velocity models shown in Figure 2. The number before the station name identifies the event, according to the map in Figure 1 and Table 1. The epicentral distances are also indicated.

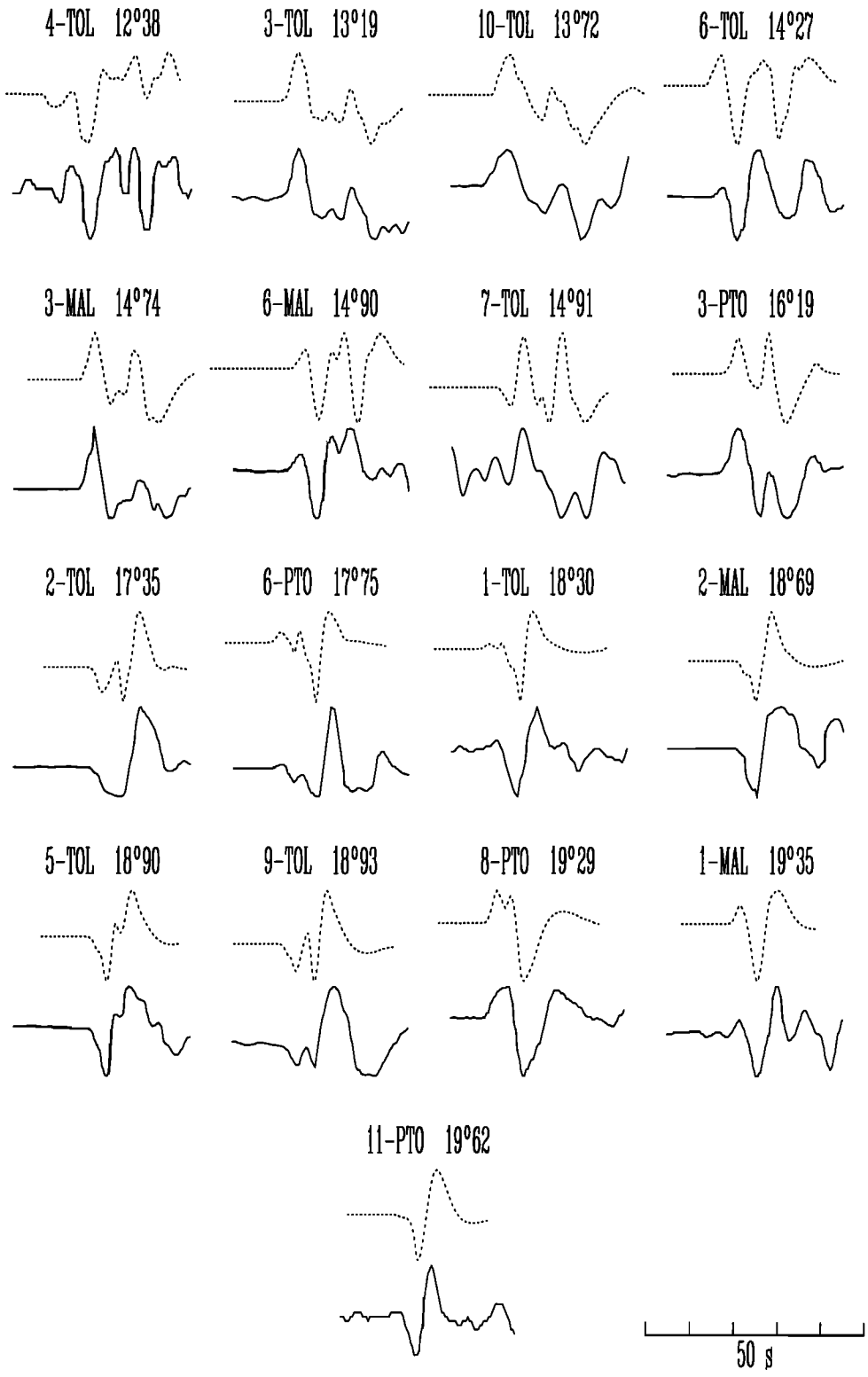

Figure 5. Comparison of WWSSN-LP waveforms with synthetic seismograms computed by using the model derived in this study (WMP2).

three stations; in fact, the azimuths to the stations, for this event, are within 20° of each other such that paths almost lay on a seismic profile. Next we have tested the results against the other event-station pairs, repeating these steps until adequate fits were obtained.

Figure 5 shows the comparison between data and synthetics computed using the velocity structure of Table 2 (each listed velocity is meant to be constant between the previous and the colisted depth). The quality of the fits is satisfactory, particularly for 3-TOL, 3-MAL, 10-TOL, and 6-MAL (event number-station name); in most cases, minor features are also reproduced. Some misfit could be due either to a low signal-to-noise ratio in the data (7-TOL) or to uncertainties in the focal mechanism. Local structure effects also can be responsible for unmatched features.

Table 2. WMP2 Model

Depth, km	Velocity, km/s	Depth, km	Velocity, km/s	Depth, km	Velocity, km/s
20	5.85	258	8.23	503	9.71
30	6.40	268	8.26	513	9.76
40	7.91	298	8.27	523	9.79
50	8.00	308	8.28	533	9.83
60	8.06	318	8.37	543	9.88
70	8.12	328	8.38	553	9.92
80	8.13	338	8.39	563	9.95
100	8.14	348	8.40	573	9.99
120	8.15	358	8.41	583	10.03
130	8.16	368	8.42	593	10.07
140	8.02	378	8.68	603	10.11
150	8.04	388	8.78	613	10.15
160	8.08	398	8.88	623	10.19
170	8.10	408	8.95	633	10.23
180	8.11	423	8.99	643	10.27
190	8.12	433	9.19	653	10.31
198	8.13	443	9.26	663	10.35
208	8.16	473	9.36	673	10.74
218	8.19	483	9.45	683	10.79
248	8.20	493	9.49	693	10.83

The new model, WMP2, is illustrated in Figure 6, together with S25, T9 and ATLP. WMP2 is very similar to ATLP within the lid, while the low velocity zone is less prominent. At intermediate depths (200-368 km) the velocity gradient is much lower than that in the other models.

Unusual features result for the discontinuity responsible for the first triplication. Several authors [see *Nolet et al.*, 1994] obtained depths around 400 km for this interface and a high-velocity jump (about 5%). In this study, no evidence has been found of such a strong discontinuity; on the contrary, an abrupt change in the velocity gradient, starting with a small discontinuity located at 368 km, is displayed by the final model. These results are justified by the slope of the C branch in the data. In Figure 7, synthetics for ATLP and WMP2 are shown along with the data: it is evident that the slowness of the C branch in the data is larger than that in the ATLP waveforms, requiring smaller velocities above the discontinuity. As a consequence, we have raised the interface in order to fit travel times. The velocity jump required at this depth to match the amplitudes is smaller than that in the other models (about 3%), but the gradient strongly increases across the interface.

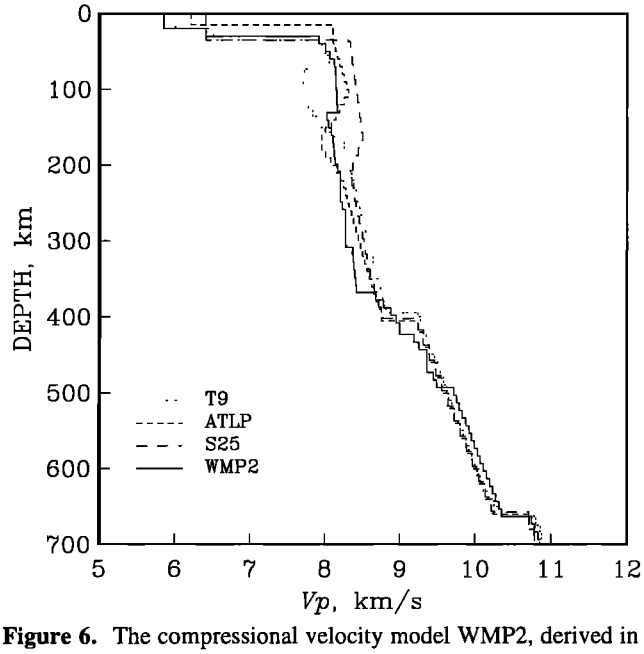

Figure 6. The compressional velocity model WMP2, derived in this study, compared with T9, ATLP, and S25.

It is important to notice that no adjustments are needed for single paths: a single model has been used for all the event-station couples. This is an indication that no major lateral variations occur perpendicular to the paths.

All but three seismograms used in this study have been recorded at epicentral distances larger than 14°. As a consequence, the effect of crustal *PL* energy on waveforms should be negligible in most of the seismograms [see *LeFevre and Helmberger*, 1989]. However, we have tested the influence of *PL* for short distance (Figure 8). To obtain these phases, we have used a reflectivity method computation in a single layered crust over a half-space. At about 13° the first pulse, formed by phases traveling in the lid and in the low-velocity zone, is not interfered with by the *PL* waves. Moreover, travel time, amplitude, and duration of the phases from the "368-km" discontinuity and below, which are the main features accounted for in the modeling procedure, are not affected by the addition of *PL* energy.

Broadband Modeling

Some broadband waveforms are also available for this region. Even though they are not enough to build an upper mantle model based on fitting of broadband waveforms alone, their major features must be accounted for by the resulting model. All the seismograms are from the broadband station installed in Toledo except one which has been recorded at the station NE11 of the temporary NARS array [*Nolet and Vlaar*, 1982]. The geographic location of these events (events 12-17) is shown in Figure 1.

Epicentral distance <20°. For this range a single seismogram

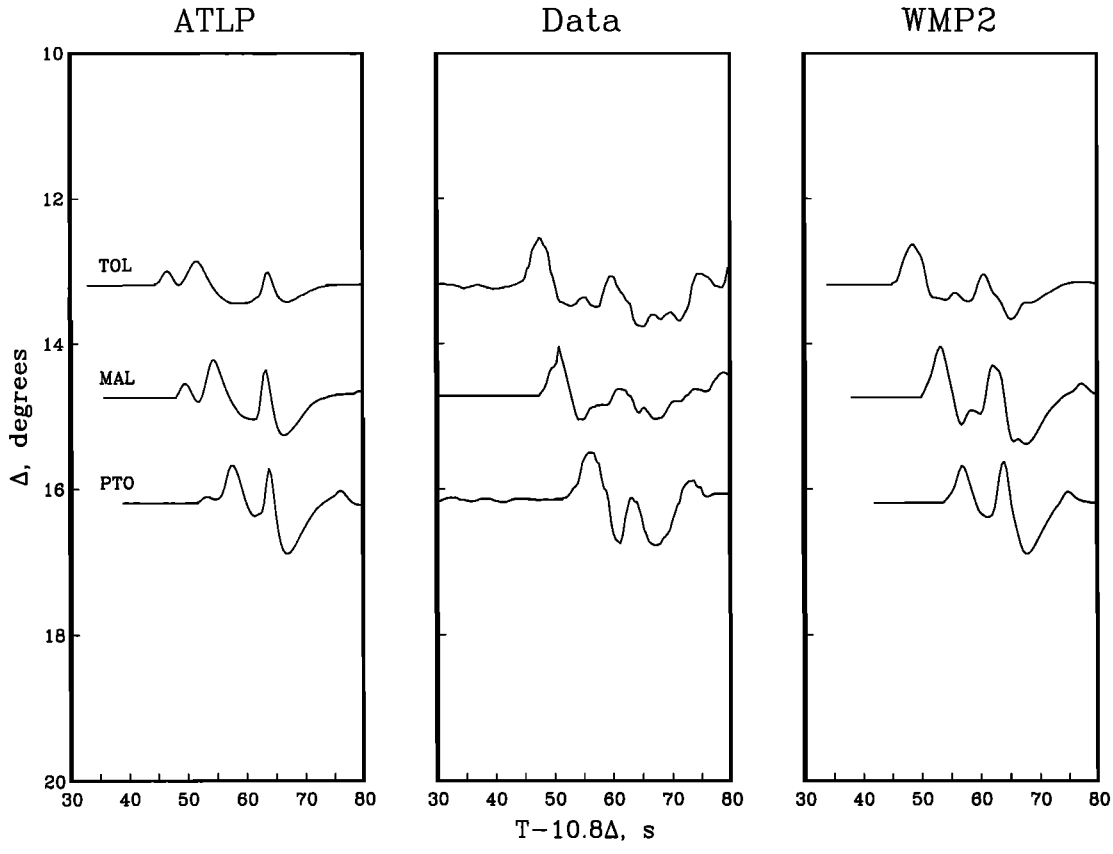

Figure 7. Synthetic waveforms predicted by ATLP and WMP2 for event 3 at TOL, MAL, and PTO compared with the data.

satisfying the previously mentioned requirements is available, and it is from an event (referred to as event 15) that occurred in southern Italy. The waveform predicted by WMP2 appears to be in very good agreement with the data (Figure 9). In particular, the long duration of the first pulse and the complex features produced on the signal by the structure around 400 km depth are confirmed in the broadband waveform.

Epicentral distance >20°. We have also included in this study five broadband seismograms, with epicentral distances larger than 20°. This range is also important to better constrain the *P* wave velocity model at intermediate depth. Rays bottoming immediately above the discontinuity at 368 km will sample this

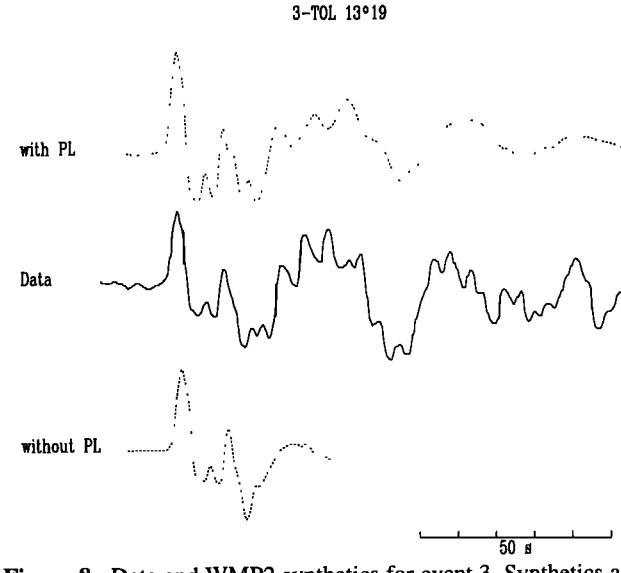

Figure 8. Data and WMP2 synthetics for event 3. Synthetics are computed both with *PL* phases included and without.

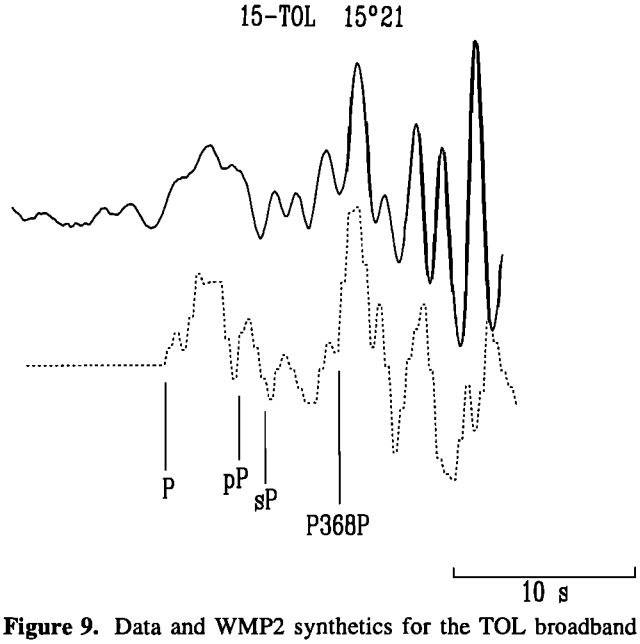

Figure 9. Data and WMP2 synthetics for the TOL broadband recording of event 15.

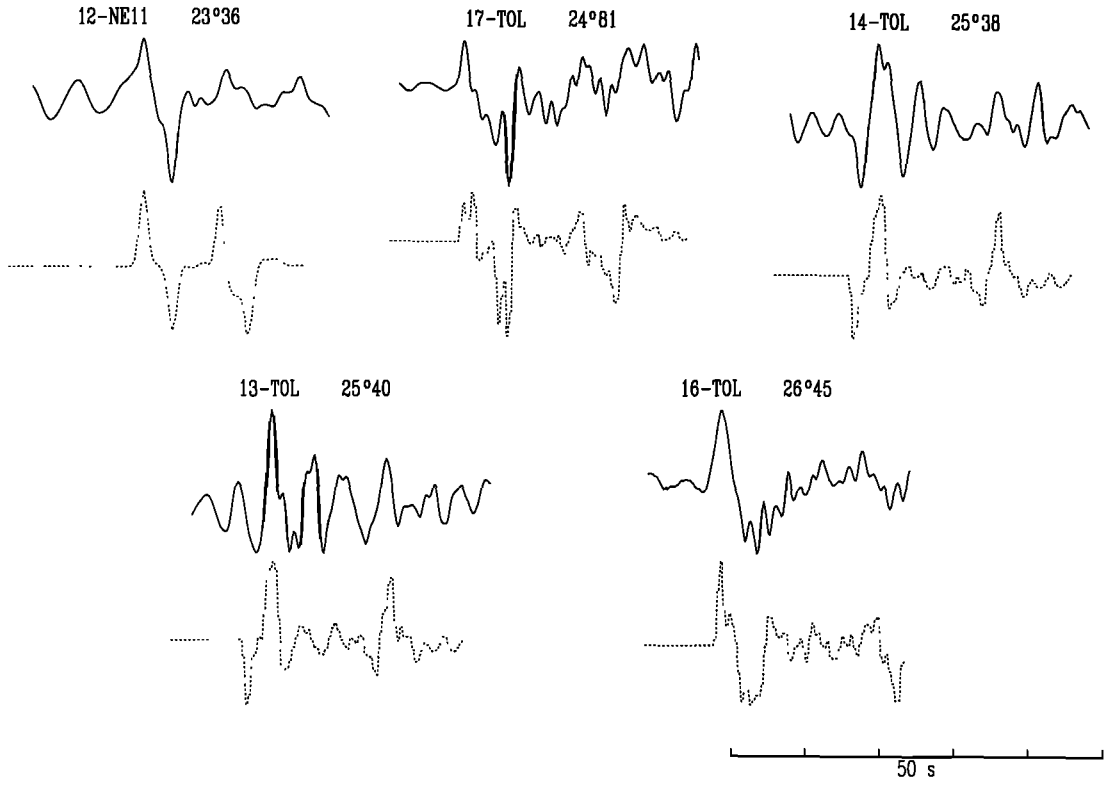

Figure 10. Data and WMP2 synthetics for the available broadband waveforms beyond 20°.

region without being affected by the discontinuity itself. These rays will produce a secondary arrival on seismograms recorded beyond 20°. Synthetic seismograms computed using WMP2 (Figure 10) correctly reproduce the features observed in the data.

Model Testing

The solution in forward modeling is nonunique; moreover, no quantitative estimation is possible for the resolution. Some test is then needed to assess the degree of approximation of the results. In this regard, we investigated the sensitivity of waveforms to various features at different depths, by computing synthetics for models derived by slightly varying WMP2. We also tested our best model against the regional average of teleseismic travel time residuals.

The Lid

In a previous section we pointed out the occurrence of a P_n branch in the data and described how this calls for the presence of a not-too-thin lid in the West Mediterranean Basin, which is also required by travel time data. We investigated the minimum lid thickness for the P_n to be generated at the examined epicentral distances. Starting from WMP2, we computed synthetics for models with progressively reduced lid thickness by 10 km, at Δ = 13°19' (3-TOL). Results, in terms of step responses, are shown in Figure 11. For values smaller than 100 km, P_n amplitude is strongly reduced, and no P_n can be detected at all for lid thickness smaller than 60 km.

The Low-Velocity Zone

The simultaneous observation of P_n and A branches is a diagnostic feature indicating the occurrence of a low velocity zone underneath the lithosphere. In this case, two distinct arrivals are distinguishable in a few waveforms and in general we interpreted the overall long pulse duration as due to a multiple arrival (see above) and modeled with a P_n phase followed by energy bottoming below a low-velocity zone. However, models with no low velocity at all (M-A) and with a thinner lid and a more pronounced low-velocity layer (M-C) (see Figure 13) were also tested, with synthetics presented in Figure 12. The occurrence of a low-velocity layer below the lid cannot be definitely assessed from this test even though the better fits obtained by using WMP2 suggest its existence.

The test of model M-C shows that a model with a thinner lid and more pronounced low-velocity layer would also give satisfactory fits to the data. The uncertainty caused by the trade-off between lid thickness and velocity in the underlying layer cannot be resolved by these data. It is also obvious that no single value for the depth of the low-velocity layer can be determined for such a complex region, while the minimum lid thickness obtained above represents a real constraint. However, it should be noted that the velocity in the low-velocity layer cannot be much lower and/or the layer itself be much thicker and satisfy the small A-P_n relative travel times.

The "368-km" Discontinuity

Above we discussed the evidence of a low apparent velocity reflection from a deep interface; a further analysis, focused on the magnitude of the velocity discontinuity and the features of the gradient above and below it, was accomplished. Figure 12 also shows synthetics computed for a model obtained from WMP2 by deepening the "368-km" discontinuity to 403 km and increasing the velocity jump to about 5% (M-B, in Figure 13); the velocity and its gradient above the interface were also increased. The

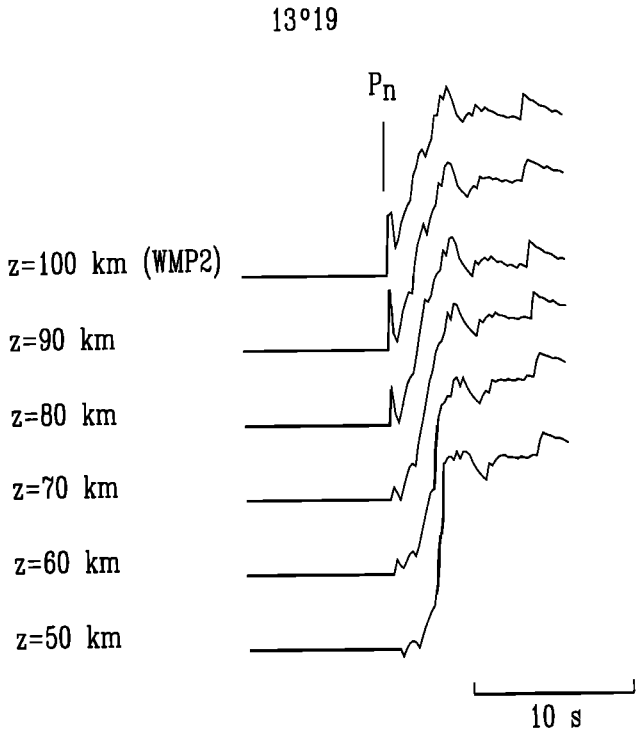

Figure 11. Step responses for the lithosphere-asthenosphere system of WMP2 and models derived by the latter by progressively reducing lid thickness z.

result was that a simple first-order discontinuity, with almost constant gradient above and below it, cannot adequately reproduce the data, as the pulses being predicted are too sharp. The same results would also be obtained if a smaller velocity gradient were used in WMP2 below the discontinuity.

Static Station Corrections

As was pointed out by *Dziewonski and Anderson* [1983, p. 3312], the azimuth independent (static) term of the station corrections "correlates with the tectonic nature of a given region . . . : the shields are fast, . . . and tectonically active regions are slow." Differences in these terms are usually ascribed to upper mantle heterogeneities. Thus models of regional upper mantle structure have to account for static station corrections.

We computed vertical travel times for the upper 500 km in the shield model KCA, derived for upper mantle structure beneath Fennoscandia by *King and Calcagnile* [1976], and in our preferred model for the West Mediterranean Basin, WMP2. The time difference WMP2-KCA is shown in Figure 14, together with static corrections for Fennoscandia and Iberian-Italian stations [*Dziewonski and Anderson*, 1983]. In the figure, KCA time is equated to the average of corrections for Scandinavian stations; ATLP, S25 and T9 vertical travel time differences relative to KCA are also plotted.

Discussion

The main features of WMP2 are as follows: a 130-km-thick lithosphere, a little pronounced low-velocity layer, a very low velocity gradient down to 368 km, where a discontinuity and a strong increase of the gradient occur. Below 500 km the model is not constrained.

Within the studied area, the lithosphere is likely to be laterally heterogeneous on a local scale. Oceanic or quasi-oceanic crust has been found in the Provençal Basin [*Hirn et al.*, 1977] and in the Tyrrhenian Sea [*Steinmetz et al.*, 1983], suggesting the existence of tectonic structures, while more transitional or continental lithosphere results in the rest of the western Mediterranean region, with a thickness of about 100 km [*Berry and Knopoff*, 1967; *Payo*, 1969; *Marillier and Mueller*, 1985]. According to these considerations, stations and events used in this study are located in continental areas, while ray paths go through oceanic structure in their central part. Thus the preferred model WMP2 represents a horizontally averaged structure throughout the studied area, with deeper layers strictly corresponding to the central part of the basin.

Our results about lithosphere structure are in very good agreement with other studies of the western Mediterranean. In particular, V_P velocities of 7.82-8.19 km/s and 8.11 km/s were found by *Bottari and Ghirlanda* [1974] and *Payo* [1969] for the lid; moreover, by inverting phase velocity curves for several paths in the West Mediterranean Basin, *Berry and Knopoff* [1967] obtained a depth of 50 ± 6 km for the roof of the low-velocity channel in the central part of the basin, between the Balearic Islands and Sardinia, rapidly dropping to 100 ± 20 km, and *Marillier and Mueller* [1985] determined the same values but with larger uncertainties. These results are quite consistent with our determination of the lid thickness. Also, the depth of the low-velocity layer in the central part of the basin is very close to the minimum depth of the lid bottom we determined by modeling the P_n phase.

As far as the asthenosphere is concerned, a well-pronounced low-velocity layer below the West Mediterranean Basin resulted in general from shear wave studies, either body wave travel time or surface wave analysis [*Berry and Knopoff*, 1967; *Payo*, 1969; *Mayer-Rosa and Mueller*, 1973; *Cara et al.*, 1980; *Panza et al.*, 1980; *Marillier and Mueller*, 1985; *Snieder*, 1988; *Zielhuis and Nolet*, 1994]. On the other hand, only a few *P* wave studies have been focused on the same region, and even though some areas of low velocity are displayed, no clear evidence of such feature being prominent and regionally extended has been found [*Payo*, 1969; *Granet and Trampert*, 1989; *Spakman et al.*, 1993]. Only in model T9 (Figure 6), derived by *Burdick* [1981] by modeling *P* waves for two Hellenic events at Iberian stations, is a distinct low compressional velocity present, but since for the Mediterranean Basin he used waveforms at epicentral distances larger than 18°, the structure above 200 km was poorly resolved.

By studying travel times for Euro-Mediterranean earthquakes, *Lehmann* [1959, 1961] pointed out the existence of a low shear velocity layer in the regional upper mantle structure, not matched by an equally evident low compressional velocity layer. She observed that unlike *S* wave, *P* wave travel times lie on a nearly straight line up to about 15°. By using a larger dataset only from events and stations located in the western Mediterranean region, merged with the results of surface wave analysis, *Payo* [1969] reached the conclusion that a low-velocity channel results from phase velocity data but not from *P* body wave travel times; he also demonstrated that *P* wave travel times could be well reproduced by a model with a constant 8.11 km/s *P* wave velocity down to a depth of 370 km.

More recently, *Granet and Trampert* [1989] and *Spakman et al.* [1993] obtained a map of *P* wave velocity anomaly for the Euro-Mediterranean region where, although patches of small negative velocity anomalies are present, no clear evidence of a regional low-velocity layer is displayed below the basin. On the

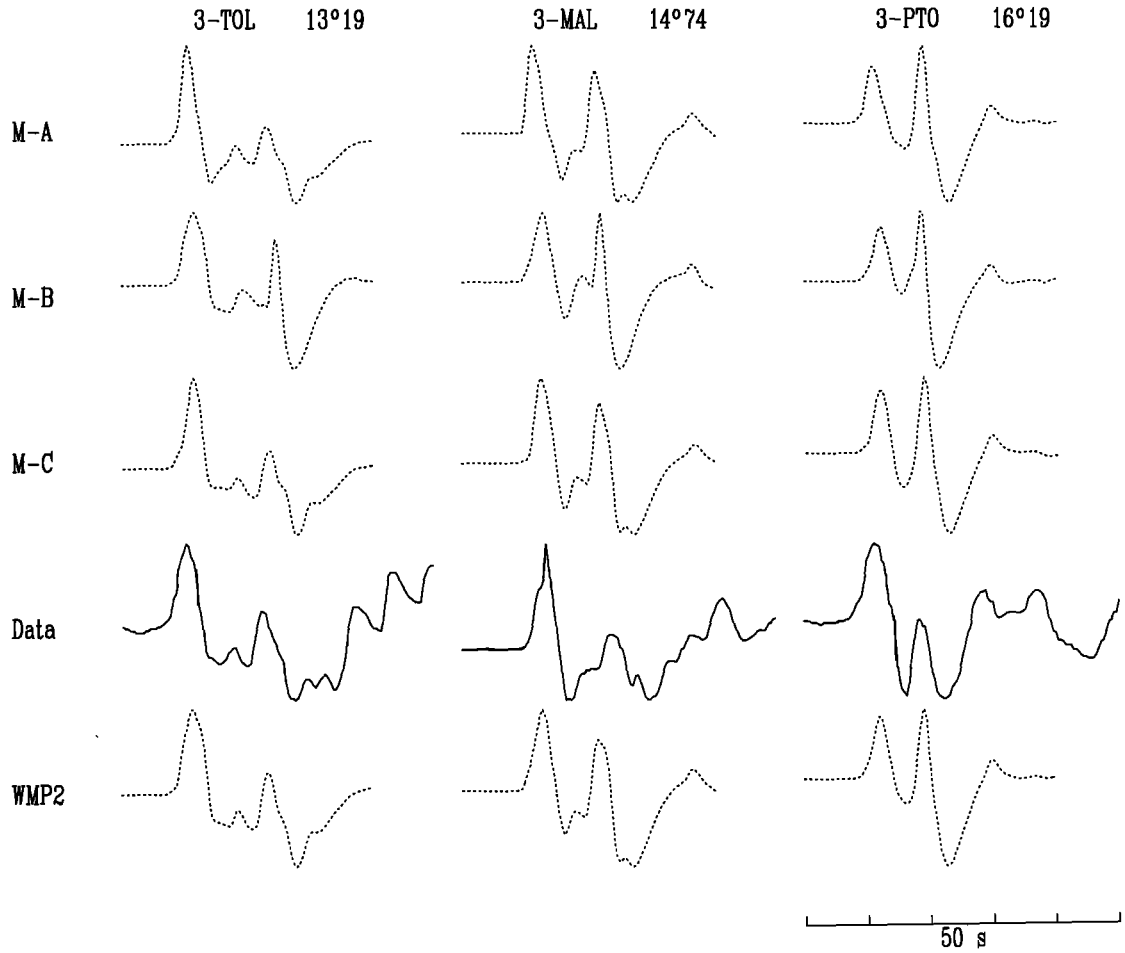

Figure 12. Comparison of waveforms predicted by WMP2, M-A, M-B, and M-C (Figure 14), along with the data.

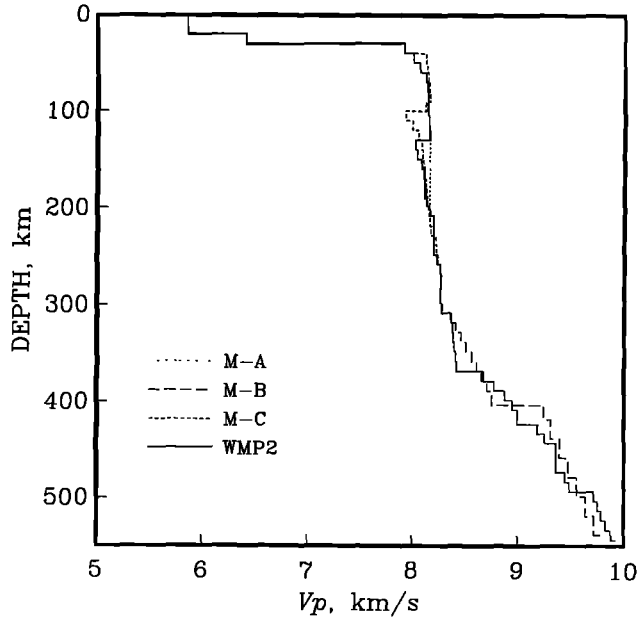

Figure 13. The preferred model WMP2, along with the models M-A, M-B, and M-C obtained by eliminating the low-velocity zone, by inserting a 5% discontinuity at 405 km and changing the velocity gradient above this depth, and by thinning the lid and enhancing the low-velocity layer, respectively.

other hand, a distinct asthenosphere always resulted in all the shear velocity studies [*Berry and Knopoff*, 1967; *Panza et al.*, 1980; *Marillier and Mueller*, 1985; *Snieder*, 1988; *Zielhuis and Nolet*, 1994]. According to *Nolet et al.* [1994], who overviewed several compressional and shear wave models for different regions, the different character of the low-velocity zone for V_P and V_S may be a global feature; they also comment that such a result is to be expected if the asthenosphere is connected to partial melting.

Assuming for the lid and the asthenosphere average shear velocities of 4.6 km/s and 4.4 km/s resulting from the mentioned studies, WMP2 would give V_P/V_S of 1.74-1.76 and 1.83-1.84, respectively. Very similar values have been obtained by *Zhao and Helmberger* [1993] for the old ocean structure in the northwestern Atlantic. On the basis of a comparison with seismic velocity computed for various petrological models by *Anderson and Bass* [1984], they hypothesized an olivine-rich mineralogy in the lithosphere and partial melting in the low-velocity layer, possibly extending down to about 300 km. These conclusions are also compatible with our results, even though lower absolute compressional velocities, with respect to ATLP, are detected below 250 km and down to 368 km.

Unusual features are displayed by WMP2 at depths between 360 and 500 km. In many regions a 5% sharp velocity discontinuity has been detected around 410 km through seismological studies (see *Bina* [1991] for a review). The data

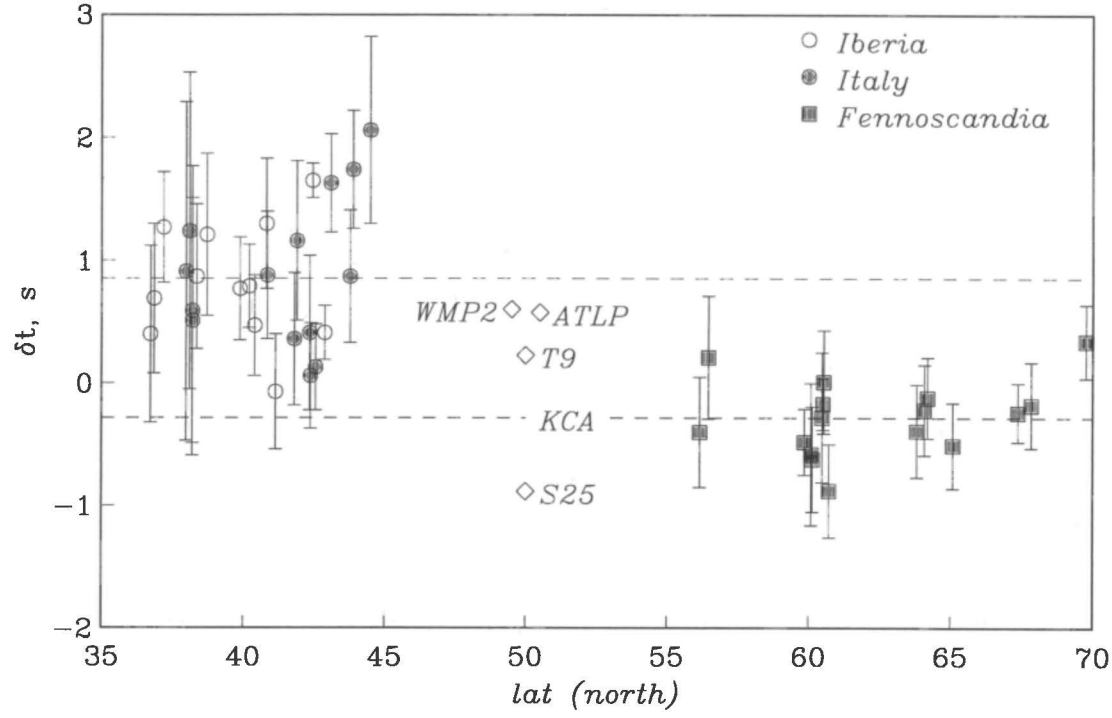

Figure 14. Static station correction for stations located in the studied area and in Fennoscandia [*Dziewonski and Anderson*, 1983] compared with the vertical travel times in several upper mantle compressional models (see text for explanation). Dashed lines correspond to average static corrections for Italian-Iberian (upper) and Fennoscandian (lower) stations.

used in this study do not present any clear indication of such a high velocity jump around 410 km, in accordance with *Spakman et al.* [1993], who explicitly notice the lack of evidence for this discontinuity in the Euro-Mediterranean region, while a 3% velocity jump results in WMP2 at 368 km depth, where the velocity gradient also increases.

It is remarkable that our best model is enclosed in a ±2% variation interval as compared to *Spakman et al.* [1993] reference model PM2 (Figure 15), which corresponds to what they obtain as a range for the velocity anomalies in the region, and the differences between WMP2 and PM2 are consistent with the results of their tomographic inversion.

Further indications about anomalous structure between 350 and 500 km depth in the West Mediterranean Basin come from the study made by *Shearer* [1993], who performed a global mapping of the upper mantle reflectors from long-period precursors to *SS* phase. In all the caps in the region analyzed here (61, 62, 89, 90) there is evidence of velocity discontinuities located at about 360 km and 490 km, while the "400 km" is absent in cap 89 and not very prominent in cap 90.

The existence of a seismic discontinuity at about 400 km depth has been known for some time. For instance, *Shearer* [1993] obtained a map of this interface on a global scale, displaying a regional topographic high of about 20 km in Eurasia, with respect to a global average of 413 km. Nevertheless, several papers have been published showing intermittency [*Paulssen*, 1988; *Nakanishi*, 1988, 1989; *Benz and Vidale*, 1993] or even absence of evidence [*Wajeman*, 1988] for such an interface.

Whether the "410-km" discontinuity involves a phase transition of an olivine-rich [*Bina and Wood*, 1987] or of a garnet-clinopyroxene-rich [*Duffy and Anderson*, 1989] isochemical mantle has been largely debated in the past. Alternatively, a chemical boundary has also been considered as a possible explanation [*Bass and Anderson*, 1984; *Anderson and Bass*, 1986]. Presently, it seems to be commonly accepted that this discontinuity is mainly due to the $\alpha \rightarrow \beta$ transition in olivine. The remaining debate concerns the amount of olivine in the upper mantle and therefore the degree to which other phase transition or chemical boundaries may contribute as well [*Jeanloz*, 1995].

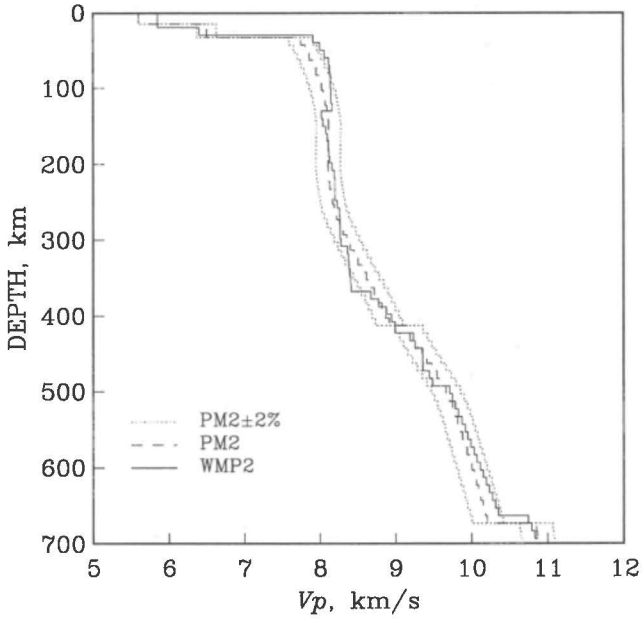

Figure 15. WMP2 compared to model PM2 [*Spakman et al.*, 1993]. The ±2% variation interval of PM2 is also drawn.

A tentative interpretation of our results in terms of an upraised olivine-to-spinel phase transition to 368 km can be made. Since both experimental studies [*Katsura and Ito*, 1989] and theoretical predictions [*Bina and Wood*, 1987] indicate a positive Clapeyron slope ($\partial P/\partial T$) for the olivine-to-spinel phase change, an increase in temperature would move the discontinuity toward deeper depths. In addition, laboratory analyses demonstrate that the thickness of the transition also varies, increasing as temperature decreases [*Katsura and Ito*, 1989] (in this case, long-period waveform studies would be more suitable in detecting undulations of the discontinuity [*Helffrich and Bina*, 1994]). As a consequence, an uplift requires lower temperatures. Unfortunately, this effect has not been observed very frequently: only a few studies have been published where travel time residuals from intermediate and deep earthquakes in subduction regions have been interpreted as being due to the elevation of the olivine-spinel phase transition [*Kaila et al.*, 1971, 1974; *Solomon and U*, 1975; *Huppert and Frolich*, 1981; *Roecker*, 1985].

In the present case, a relatively cold upper mantle might be hypothesized in connection with the north dipping subduction of the African plate depicted by tectonic reconstructions made, for instance, by *Dercourt et al.* [1986] and *Dewey et al.* [1989]. These authors suggest that convergence between Eurasia and Africa has been taking place since late Cretaceous (80 Myr according to *Dercourt et al.* [1986], 92 Myr according to *Dewey et al.* [1989]) with some variation in the direction and velocity of the relative motion. Presently, a roughly NS shortening results in the basin area [*Westaway*, 1992]; also some intermediate (<150 km) and three deep (>600 km) earthquakes occurred in the last 50 years, in the Alboran Sea region [*Buforn et al.*, 1991], and a clear tomographic image of a subducted slab has been obtained by *Blanco and Spakman* [1993].

However different, both these reconstructions predict a north dipping subducted slab in the West Mediterranean Basin at least 400-500 km long which is also detected by tomographic studies [*De Jonge et al.*, 1994].

Assuming the value of 2.5 MPa K^{-1}, estimated by *Fei et al.* [1991] for the Clapeyron slope, and a normal depth of 393 km in this region, from the mentioned study by *Shearer* [1993], in order to raise the discontinuity by 25 km, a decrease of about 300°C is required. As compared to other models (Figure 6), the smaller velocity jump might be explained by the smearing of the discontinuity over a broader interval, resulting from lower temperatures, as mentioned above. Such a temperature decrease could be accounted for by a slab structure penetrating the whole upper mantle, like the one predicted in this region [*De Jonge et al.*, 1994].

The occurrence of low temperatures is apparently contradicted by the low velocities displayed by WMP2. Actually, many studies carried out in subduction zones show similar results. For instance, *Kaila et al.* [1971] found *P* wave velocities very similar to those of WMP2 (8.52 km/s at a depth of 365 km, where a strong discontinuity occurs), *Van der Hilst et al.* [1991] found low-*P* velocity anomalies down to a depth of 400 km below some northwestern Pacific island arcs, which in some cases (Izu Bonin) are as large as -5%, relative to IASP91, and *Revenaugh and Sipkin* [1994] found a decreasing impedance below 330 km from analysis of *ScS* reverberations in the northwestern Pacific subduction zone. In addition, very low *S* velocity has been detected by *Zielhuis and Nolet* [1994], from shear and surface waveform inversion, below the continental boundary marked by the Tornquist-Teisseyre zone (eastern Europe).

Low velocities in the upper mantle are usually explained by the presence of melt along the mantle-slab interface in the wedge, or of fluid from dehydration process in the slab [*Ringwood*, 1974; *Fyfe and McBirney*, 1975; *Wyllie*, 1982; *Hsui et al.*, 1983]. These processes were traditionally considered as taking place at depths of less than 200 km, but in the last 15 years the idea that a considerable amount of water can be present down to the transition zone has been commonly accepted [*Thompson*, 1992].

In their extensive analysis, attempting to explain the low velocity at depth, *Nolet and Zielhuis* [1994] remark that water involved in subduction can generate considerable quantities of partial melt. This melt would be more dense than olivine, at upper mantle pressure, and then would not migrate upward [*Miller et al.*, 1991; *Agee and Walker*, 1993]. By conservative computation, they also conclude that a subduction episode lasting 85 Myr would accumulate enough water at depth to explain the occurrence of the low velocities. This is exactly what is thought to be the age of subduction in the West Mediterranean Basin (see above).

A negatively buoyant silicate melt is also the key to an alternative interpretation of our results. The low reflectivity below 318 km in WMP2 could be connected to the presence of such melt. In these circumstances, the 368 km would be the bottom end of this layer, giving rise to a strong reflection partially masking the possibly occurring "410 km," which in WMP2 would be the small jump at about 420 km. This explanation is similar to what *Revenaugh and Jordan* [1991] claim to be the cause for the X discontinuity they detect in some western Pacific subduction areas.

From our results, there is no reason to prefer either interpretation, both being absolutely consistent with the data. However, the occurrence of low velocity below 300 km requires the presence of dense melt produced by abundant water which, in turn, is connected to subduction.

Conclusions

By waveform modeling, we have developed a one-dimensional model for the upper mantle compressional velocity structure in the West Mediterranean Basin. Although we considered paths through a complex tectonic environment, detailed information has been obtained, especially as regards the deep structure of the basin. This confirms that, as *Nolet et al.* [1994] pointed out, when insufficient data density is available, which is the case in the basin area, one-dimensional modeling very often provides more robust results than three-dimensional studies.

The preferred model, WMP2, represents an average structure along the paths under consideration and is very useful as a reference for tomographic inversion. It displays a lid about 100 km thick over a not very pronounced low-velocity layer and a 3% discontinuity at 368 km. The latter has been tentatively interpreted as the olivine-to-spinel transition, regionally detected at about 395 km, deflected by the lower temperature caused by the subduction of the African plate or, alternatively, as being due to the presence of a layer of silicate melt below 300 km depth, producing a strong reflection from its bottom, and a more usual depth of 420 km for the olivine-spinel transition. In both cases the occurrence of relatively low velocities at depth beneath 300 km, caused by melt or fluid, is to be considered.

Ackowledgments. N. A. P. wishes to thank all the people at the Seismolab, faculty, staff, and students, who made his nine-month stay a very pleasant experience.

References

Agee, C.B., and D. Walker, Olivine flotation in the mantle melt, *Earth Planet. Sci. Lett.*, *114*, 315-324, 1993.

Amato, A., B. Alessandrini, and G.B. Cimini, Teleseismic wave tomography of Italy, in *Seismic Tomography: Theory and Methods*, edited by H.M. Iyer and K. Hirahara, 361-397, Chapman and Hall, New York, 1993.

Anderson, D.L., and J.D. Bass, Mineralogy and composition of the upper mantle, *Geophys. Res. Lett.*, *11*, 637-640, 1984.

Anderson, D.L., and J.D. Bass, Transition region of the Earth's upper mantle, *Nature*, *320*, 321-328, 1986.

Anderson, H., and J. Jackson, Active tectonics of the Adriatic region, *Geophys. J. R. Astron. Soc.*, *91*, 937-984, 1987.

Bass, J.D., and D.L. Anderson, Composition of the upper mantle: Geophysical tests of two petrological models, *Geophys. Res. Lett.*, *11*, 237-240, 1984.

Benz, H., and J. Vidale, Sharpness of upper-mantle discontinuities determined from high frequency reflections, *Nature*, *365*, 147-150, 1993.

Berry, M.J., and L. Knopoff, Structure of the upper mantle under the western Mediterranean Basin, *J. Geophys. Res*, *72*, 3613-3636, 1967.

Bina, C.R., Mantle discontinuities, *U.S. Natl. Rep Int Union Geod. Geophys. 1987-1990, Rev. Geophys.*, *29*, 783-793, 1991.

Bina, C.R., and B.J. Wood, Olivine-spinel transition: Experimental and thermodynamic constraints and implications for the nature of the 400-km seismic discontinuities, *J. Geophys. Res.*, *92*, 4853-4866, 1987.

Blanco, M.J., and W. Spakman, The *P*-wave velocity structure of the mantle below the Iberian Peninsula: Evidence for a subducted lithosphere below southern Spain, *Tectonophysics*, *176*, 137-165, 1993.

Bottari, A., and A. Ghirlanda, Some results for the middle western Mediterranean Basin from the study of P_n waves, *Bull. Seismol. Soc. Am.*, *64*, 427-435, 1974.

Buforn, E., A. Udias, and R. Madariaga, Intermediate and deep earthquakes in Spain, *Pure Appl. Geophys.*, *136*, 375-393, 1991.

Burdick, L.J., A comparison of upper mantle structure beneath North America and Europe, *J. Geophys. Res.*, *86*, 5926-5936, 1981.

Cara, M., A. Nercessian, and G. Nolet, New inferences from higher mode data in western Europe and northern Eurasia, *Geophys. J. R. Astron. Soc.*, *61*, 459-478, 1980.

Cocco, M., and A. Rovelli, Evidence for the variation of stress drop between normal and thrust faulting earthquakes in Italy, *J. Geophys. Res.*, *94*, 9399-9416, 1989.

De Jonge, M.R., M.J.R. Wortel, and W. Spakman, Regional scale tectonic evolution of the lithosphere and upper mantle: The Mediterranean region, *J. Geophys. Res.*, *99*, 12091-12108, 1994.

Dercourt, J., et al., Geological evolution of the Tethys Belt from the Atlantic to the Pamirs since the Lias, *Tectonophysics*, *123*, 241-315, 1986.

Dewey, J.F., M.L. Helman, E. Turco, D.H.W. Hutton, and S D. Knott, Kinematics of the western Mediterranean, in Alpine Tectonics, edited by M.P. Coward, D. Dietrich, and R.G. Park, *Geol. Soc. Spec. Publ.*, *45*, 265-283, 1989.

Duffy, T.S., and D.L. Anderson, Seismic velocities in mantle minerals and the mineralogy of the upper mantle, *J. Geophys. Res.*, *94*, 1895-1912, 1989.

Dziewonski, A.M., and D.L. Anderson, Travel times and station corrections for *P* waves at teleseismic distances, *J. Geophys. Res.*, *88*, 3295-3314, 1983.

England, P.C., and M.H. Worthington, The travel time of *P* seismic waves in Europe and western Russia, *Geophys. J. R. Astron. Soc.*, *48*, 63-70, 1977.

Fei, Y., H.-K. Mao, and B.O. Mysen, Experimental determination of element partitioning and calculation of phase relations in the MgO-FeO-SiO_2 system at high pressure and high temperature, *J. Geophys. Res.*, *96*, 2157-2169, 1991.

Futtermann, W.I., Dispersive body waves, *J. Geophys. Res.*, *67*, 5279-5291, 1962.

Fyfe, W.S., and A.R. McBirney, Subduction and the structure of andesitic volcanic belts, *Am. J. Sci.*, *275-A*, 285-297, 1975.

Geiss, E., A new compilation of crustal thickness data for the Mediterranean area, *Ann. Geophys., Ser. B*, *5*, 623-630, 1987.

Grand, S.P., and D.V. Helmberger, Upper mantle shear structure beneath the northwest Atlantic Ocean, *J. Geophys. Res.*, *89*, 11465-11475, 1984.

Granet, M., and J. Trampert, Large-scale *P*-velocity structures in the Euro-Mediterranean area, *Geophys. J. Int.*, *99*, 583-594, 1989.

Helffrich, G., and C.R. Bina, Frequency dependence of the visibility and depths of mantle seismic discontinuities, *Geophys. Res. Lett.*, *21*, 2613-2616, 1994.

Helmberger, D.V., Long period body wave propagation from 4° to 13°, *Bull. Seismol. Soc. Am.*, *62*, 325-341, 1972.

Helmberger, D.V., Theory and application of synthetic seismograms, in *Earthquake: Observations, Theory and Interpretation*, edited by H. Kanamori and E. Boschi, *Proc. Int. Sch. Phys. Enrico Fermi*, *85*, 174-222, 1983.

Hirn, A., L. Steinmetz, and M. Sapin, A long range seismic profile in the western Mediterranean Basin: Structure of the upper mantle, *Ann. Geophys.*, *33*, 373-384, 1977.

Hsui, A.T., B.D. Marsh, and M.N. Toksöz, On melting of the subducted oceanic crust: Effect of subduction induced mantle flow, *Tectonophysics*, *99*, 207-220, 1983.

Huppert, L.W., and C. Frolich, The *P* velocity within the Tonga Benioff zone determined from traced rays and observations, *J Geophys. Res.*, *86*, 3771-3782, 1981.

Ita, J., and L. Stixrude, Petrology, elasticity, and composition of the mantle transition zone, *J. Geophys. Res.*, *97*, 6849-6866, 1992.

Jeanloz, R., Earth dons a different mantle, *Nature*, *378*, 130-131, 1995.

Kaila, K.L., V.G. Krishna, and H. Narain, Upper mantle *P*-wave velocity structure in the Japan region from travel-time studies of deep earthquakes using a new analytical method, *Bull. Seismol. Soc Am.*, *61*, 1549-1570, 1971.

Kaila, K.L., V.G. Krishna, and H. Narain, Upper mantle shear-wave velocity structure in the Japan region, *Bull. Seismol. Soc. Am.*, *64*, 355-374, 1974.

Katsura, T., and E. Ito, The system Mg_2SiO_4-Fe_2SiO_4 at high pressures and temperatures: Precise determination of stabilities of olivine, modified-spinel, and spinel, *J. Geophys. Res.*, *94*, 15663-15670, 1989.

King, D.W., and G. Calcagnile, *P*-wave velocities in the upper mantle beneath Fennoscandia and western Russia, *Geophys. J. R. Astron. Soc.*, *46*, 407-432, 1976.

LeFevre, L.V., and D.V. Helmberger, Upper mantle *P* velocity of the Canadian shield, *J. Geophys. Res.*, *94*, 17749-17765, 1989.

Lehmann, I., Velocities of longitudinal waves in the upper part of the Earth's mantle, *Ann. Geophys.*, *15*, 93-118, 1959.

Lehmann, I., *S* and the structure of the upper mantle, *Geophys. J. R. Astron. Soc.*, *4*, 124-138, 1961.

Marillier, F., and S.T. Mueller, The western Mediterranean region as an upper-mantle transition zone between two lithospheric plates, *Tectonophysics*, *118*, 113-130, 1985.

Mayer-Rosa, D., and S.T. Mueller, The gross velocity-depth distribution of *P*- and *S*-waves in the upper mantle of Europe from earthquake observations, *Z. Geophys.*, *39*, 395-410, 1973.

Miller, G.H., E.M. Stolper, and T.J. Ahrens, The equation of state of a molten komatiite, 1, Shock wave compression to 36 GPa, *J. Geophys. Res.*, *96*, 11831-11848, 1991.

Nakanishi, I., Reflections of *P'P'* from upper mantle discontinuities beneath the Mid-Atlantic Ridge, *Geophys. J. Int.*, *93*, 335-346, 1988.

Nakanishi, I., A search for topography of the mantle discontinuities from precursors to *P'P'*, *J. Phys. Earth*, *37*, 297-301, 1989.

Nolet, G., and N.J. Vlaar, The NARS project: Probing the Earth's interior with a large seismic antenna, *Terra Cognita*, *2*, 17-25, 1982.

Nolet, G., and A. Zielhuis, Low-*S* velocities under the Tornquist-Teisseyre zone: Evidence for water injection into the transition zone by subduction, *J. Geophys. Res.*, *99*, 15813-15820, 1994.

Nolet, G., S.P. Grand, and B.L.N. Kennett, Seismic heterogeneity in the upper mantle, *J. Geophys. Res.*, *99*, 23753-23766, 1994.

Panza, G.F., S.T. Mueller, and G. Calcagnile, The gross features of the lithosphere-asthenosphere system in Europe from seismic surface waves and body waves, *Pure Appl. Geophys.*, *118*, 1209-1213, 1980.

Papazachos, C., and G. Nolet, *P* and *S* deep velocity structure of the Hellenic area obtained by robust nonlinear inversion of travel times, *J. Geophys. Res.*, in press, 1997.

Paulssen, H., Lateral heterogeneity of Europe's upper mantle as inferred from modelling of broad-band body waves, *Geophys. J. R. Astron. Soc.*, *91*, 171-199, 1987.

Paulssen, H., Evidence for a sharp 670-km discontinuity as inferred from *P*-to-*S* converted waves, *J. Geophys. Res.*, *93*, 10489-10500, 1988.

Payo, G., Crustal structure of the Mediterranean Sea, part I, Group velocities, *Bull. Seismol. Soc. Am.*, *57*, 151-172, 1967.

Payo, G., Crustal structure of the Mediterranean Sea, part II, Phase velocities and travel times, *Bull. Seismol. Soc. Am.*, *59*, 23-42, 1969.

Revenaugh, J., and T.H. Jordan, Mantle layering from *ScS* reverberations, 3, The upper mantle, *J. Geophys. Res.*, *96*, 19781-19810, 1991.

Revenaugh, J., and S.A. Sipkin, Seismic evidence for silicate melt atop the 410-km mantle discontinuity, *Nature*, *369*, 474-476, 1994.

Ringwood, A.E., The petrological evolution of island arc systems, *J. Geol. Soc. London*, *130*, 183-204, 1974.

Roecker, S.W., Velocity structure in the Izu-Bonin seismic zone and the depth of the olivine-spinel phase transition in the slab, *J. Geophys. Res.*, *90*, 7771-7794, 1985.

Romanowicz, B.A., A study of large-scale lateral variations of *P* velocity in the upper mantle beneath western Europe, *Geophys. J. R. Astron. Soc.*, *63*, 217-232, 1980.

Scarpa, R., Travel time residuals and three-dimensional velocity structure of Italy, *Pure Appl. Geophys.*, *120*, 583-606, 1982.

Shearer, P.M., Global mapping of upper mantle reflectors from long-period *SS* precursors, *Geophys. J. Int.*, *115*, 878-904, 1993.

Snieder, R., Large waveform inversions of surface waves for lateral heterogeneity, 2, Application to surface waves in Europe and the Mediterranean, *J. Geophys. Res.*, *93*, 12067-12080, 1988.

Solomon, S.C., and K.T.P. U, Elevation of the olivine-spinel transition in subducted lithosphere: Seismic evidence, *Phys Earth Planet. Inter.*, *11*, 97-108, 1975.

Spakman, W., Delay-time tomography of the upper mantle below Europe, the Mediterranean, and Asia minor, *Geophys. J. Int.*, *107*, 309-332, 1991.

Spakman, W., S. Van der Lee, and R. Van der Hilst, Travel-time tomography of the European-Mediterranean mantle down to 1400 km, *Phys. Earth Planet. Inter.*, *79*, 3-74, 1993.

Steinmetz, L., F. Ferrucci, A. Hirn, C. Morelli, and R. Nicolich, A 50 km long Moho traverse in the Tyrrhenian Sea from OBS recorded P_n waves, *Geophys. Res. Lett.*, *10*, 428-431, 1983.

Thompson, A.B., Water in the Earth's upper mantle, *Nature*, *358*, 295-302, 1992.

Van der Hilst, R., R. Engdahl, W. Spakman and G. Nolet, Tomographic imaging of subducted lithosphere below northwest Pacific islands arc, *Nature*, *353*, 37-43, 1991.

Wajeman, N., Detection of underside *P* reflection at mantle discontinuities by stacking broadband data, *Geophys. Res. Lett.*, *15*, 669-672, 1988.

Westaway, R., Seismic moment summation for historical earthquakes in Italy: Tectonic implications, *J. Geophys. Res.*, *97*, 15437-15464, 1992.

Wyllie, P.J., Subduction products according to experimental prediction, *Geol. Soc. Am. Bull.*, *93*, 468-476, 1982.

Zhao, L.S., and D.V. Helmberger, Upper mantle compressional velocity structure beneath the northwest Atlantic Ocean, *J. Geophys. Res.*, *98*, 14185-14196, 1993.

Zielhuis, A., and G. Nolet, Shear-wave velocity variations in the upper mantle beneath central Europe, *Geophys. J. Int.*, *117*, 695-715, 1994.

D.V. Helmberger, California Institute of Technology, Seismological Laboratory 252-21, Pasadena, CA 91125. (email@helm.seismo.gps.caltech.edu)

N.A. Pino, Istituto Nazionale di Geofisica, Via di Vigna Murata 605, 00143 Rome, Italy. (e-mail: pino@marte.ingrm.it)

(Received April 30, 1996; revised October 25, 1996;
accepted November 6, 1996.)